Target Density Fluctuation Monitoring in the HAPPEX Helium Parity Violation Experiment

Lindsay Glesener
San Francisco State University
Advisor: Prof. David Armstrong
College of William and Mary

August 5, 2005

Abstract

Luminosity monitors were used to study density fluctuations in the cold helium-4 target of the HAPPEX-He parity violation experiment in Jefferson Lab Hall A. Helicity-correlated asymmetries were measured as beam current, beam raster size, target fan speed, and target density were varied. These studies were used to determine optimal running conditions and estimate the contribution of target density fluctuations to the statistical error of the experiment.

1 Introduction

The summer 2004 run of the Happex-He experiment in Hall A of Jefferson Lab was limited to an electron beam current of 35 μA [1]. Reasons for this included density fluctuations in the cryogenic helium target. These fluctuations, which were large at currents higher than 35 μA, increased the statistical error of the experiment.

For the summer 2005 run of Happex-He, tests were conducted to determine the extent of the target density fluctuations. The goal of these tests was to find target and beam configurations which minimized density fluctuations. This would allow use of a higher beam current, which in turn would increase statistical accuracy because of a higher scattering rate. Two sets of luminosity monitors, which were not sensitive to parity violating asymmetries, were used to measure asymmetry widths due to target density fluctuations.

2 Overview

2.1 Helium Target

The Happex-He experiment uses a 20 cm cryogenic helium-4 gas target. The target is cryogenically cooled to a temperature of 6.4 to 6.7 degrees kelvin and

is kept at a pressure of 200 to 212 psi and a density of 0.136 g/cm^3 (with the exception of some low-density tests described later). Cold helium gas is circulated throughout the thin-walled aluminum cell by a fan operating at frequencies between 20 and 70 Hz. A high power heater compensates for changes in the target temperature due to fluctuations in beam current and cryogenic flow.

2.2 Electron Beam

The experiment uses a continuous 2.751 GeV electron beam supplied by CEBAF, the continuous electron beam accelerator facility at Jefferson Lab. Current up to 100 μA is available. The beam is rastered to avoid concentrated heating of the target cell.

Happex-He is a parity violation experiment using an electron beam with up to 85% polarization [2][3]. The scattering rate of electrons off the target nuclei depends on the electrons' helicity, or relative orientation of electron spin and momentum (parallel or antiparallel). Beam helicity is controlled by illuminating electrons with right or left circularly polarized laser light. The helicity of the beam is configured in "window pairs," with each window lasting 33.3 ms. The first window in the pair consists of a pseudorandomly chosen helicity and is followed by a second window of opposite helicity. The asymmetry, discussed later, is determined by comparing electron scattering rates for the two beam helicities [2].

3 Monitoring Density Fluctuations

3.1 Luminosity Monitor Location

Two sets of luminosity monitors (or "Lumis") are located on the beamline in Hall A. The "back lumis" are a set of eight Lumis installed directly into the beamline 7 m downstream from the target. These Lumis were first used in the 2004 run of Happex and are staggered slightly in the direction of the beam pipe so as not to stress it (see Figure 1). The scattering angle seen by these Lumis is 0.5° to 0.8° [4].

The two "forward Lumis" are located on stands on either side of the target chamber at a scattering angle of 45° and a distance of 1 m. These Lumis were used in the previous Happex-I and Happex-II experiments[5] and were reinstalled just before target cooldown. Because of their proximity to the target, the PMT's of the forward Lumis are shielded by lead to avoid radiation damage. In addition, these Lumis are covered by plastic to avoid moisture from condensation on the cryogenic pipes. Because of the large scattering angle (and therefore few scattered electrons) at this location, the asymmetry widths measured by these Lumis are large.

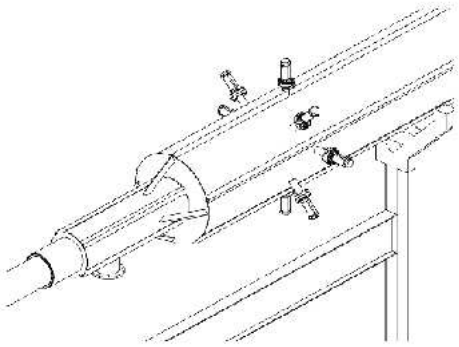

Figure 1: The "back Lumis," located 7 m downstream of the target at a scattering angle of 0.5° to 0.8° [4].

Figure 2: Quartz Čerenkov detector used in the luminosity monitors [2]

3.2 Luminosity Monitor Components

Each Lumi monitor includes a rectangular detector of synthetic quartz (SiO2: Spectrosil 2000) with a refractive index homogeneity of 10×10^{-6} [6] (see figure 2). Čerenkov light is detected in the quartz and carried away from the electron beam via an aluminum-walled cylindrical light guide [7]. The light guide is connected to an 8-stage R7723 photomultiplier tube (PMT) [7]. Electrical tape is used to shield the entire device from background light, and a flow of nitrogen is supplied to the photomultiplier tube to counteract the effects of external helium gas present in the experimental hall, which could otherwise leak into the PMTs and interfere with their signals [8].

The output signal from the PMT is directed to a 16-bit integrating analog-to-digital converter (ADC), which feeds into the experimental data acquisition software.

4 Procedure

The 2005 Happex-He experiment began running on July 16. Data from the Lumis were taken periodically over the next two weeks to determine the extent of target density fluctuations for different configurations of the beam and the

target. The variables that were varied included beam current, beam raster size, target fan speed, and target density and temperature.

The raw Lumi ADC values from each helicity window were used to calculate the asymmetry [1]:

$$A = \frac{N_R - N_L}{N_R + N_L}$$

N_R denotes detected scattering of electrons with spin and momentum parallel (right-handed) and N_L denotes detected scattering of electrons with spin and momentum antiparallel. The asymmetries were normalized to those from beam current monitors to correct for current asymmetries that existed in the beam before scattering. The asymmetries were then regressed against beam position monitors located in Hall A and the beam switchyard to correct for changes in beam position and energy. This was done by means of a linear fit of Lumi asymmetries to beam position monitor differences and a subsequent subtraction of this slope.

The statistical widths of the asymmetry distributions were analyzed. If no broadening of the asymmetry widths were present, the widths should follow a Poisson distribution with $\sigma_n = \sqrt{n}$ [9]. The deviation of the widths from counting statistics in all Lumis indicated the presence of target density fluctuations. The eight back Lumis are especially useful for this purpose because the small scattering angle at which they are located does not allow them to detect the physics asymmetry of the experiment. Most of the reported analysis will focus on these monitors.

While the raw ADC values depend on the high voltage supplied to the PMT, the widths of the asymmetry distributions should be independent of the high voltages supplied to the Lumis. This was confirmed by Happex experimenters in fall 2002 [5].

4.1 Variables Tested

4.1.1 Current

To determine the restrictions on electron beam current by target density fluctuations, back Lumi asymmetry widths were measured for currents between 4 and 40 μA. Beam-induced heating of magnets in the main spectrometers did not allow testing at currents over 40 μA.

Lumi asymmetry widths were then compared to those predicted by counting statistics. Since scattered electrons are proportional to beam current, asymmetry widths should decrease as $\frac{1}{\sqrt{I}}$.

4.1.2 Fan Speed and Target Density

A fan circulates cold helium gas throughout the target cell. Back Lumi widths were measured for fan frequencies of 24 Hz to 60 Hz. In addition, the density of the target was manipulated by bleeding off helium. Fan speed tests were done at three different densities: 0.136 g/cm^3, 0.116 g/cm^3, and 0.083 g/cm^3.

4.1.3 Beam Raster Size

In order to avoid intense heating of one area of the target cell by a concentrated, narrow electron beam, the Happex experiment uses a beam raster. The raster spreads out the electron beam, lowering the power density deposited on the target. The size of the raster has been observed before to have an effect on target density fluctuations [5], and so back Lumi asymmetry widths were compared for three different raster sizes from 9 mm^2 to 49 mm^2. This test was repeated for a lower density target.

5 Results

5.1 Current

Figure 3 shows the asymmetry widths measured by each Lumi monitor for a current scan of 10 μA to 40 μA. The smooth black line denotes the widths expected by counting statistics. The widths deviate from counting statistics immediately as the current rises, indicating that target density fluctuations increase quickly with current. This data was taken with a fan speed of 38 Hz and a 7 mm x 7 mm raster.

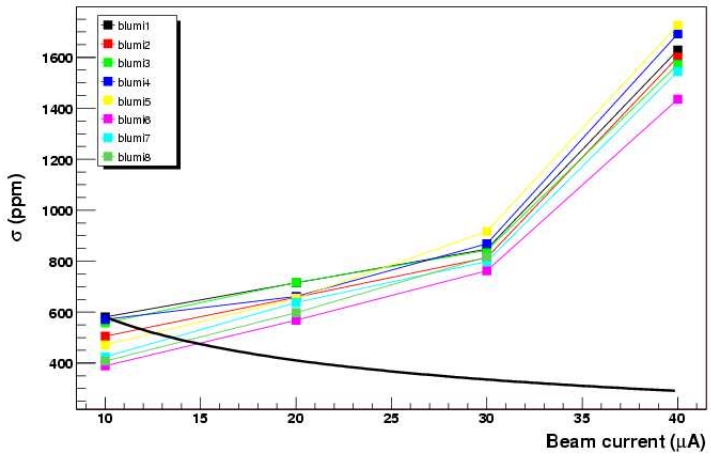

Figure 3: Lumi asymmetry widths vs. current for a fan speed of 38 Hz and a 7mm x 7mm raster. The black line indicates results expected by counting statistics.

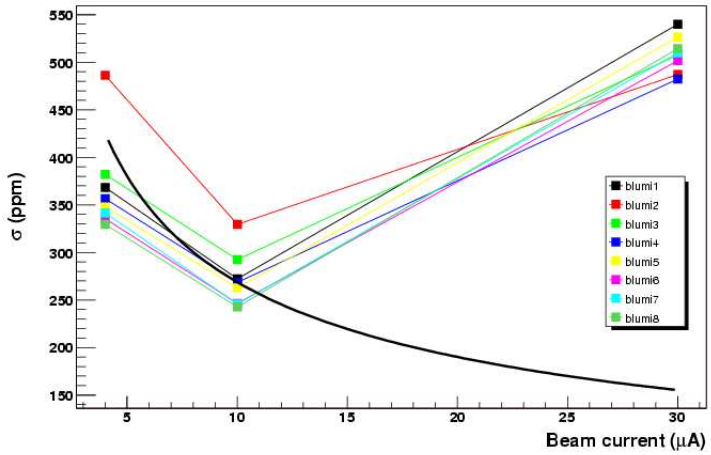

Figure 4: Lumi asymmetry widths vs. current for a fan speed of 60 Hz and a 7mm x 7mm raster. The black line indicates results expected by counting statistics.

Figure 4 shows Lumi asymmetry widths for a current scan of 4 μA to 30 μA. The fan speed was higher than that of the last current scan, resulting in smaller widths. This figure shows that at low current (4 μA to 10 μA) the widths do decrease with current, although not enough to be explained completely by counting statistics. Above 10 μA, density fluctuations quickly escalate. The counting statistics line has been normalized to a Lumi width at 10 μA. This was done because the number of scattered electrons at 4 μA is small and thus the distribution begins to look non-Gaussian.

Figure 5 shows the widths seen by the Lumis for the same current scan. The points represent a combined width for all eight back Lumis and were determined by the following:

$$\frac{1}{\sigma^2_{combined}} = \Sigma \frac{1}{\sigma^2_i}$$

The combined Lumi widths do not scale to the counting statistics line because of the presence of target density fluctuations. Assuming that at 10 μA (with a fan speed of 60 Hz, and a 7mm x 7mm raster) pure statistical widths are being measured, the amount of density fluctuation at 30 μA can be estimated. At 10 μA, the combined Lumi asymmetry width is 210 ppm. It is expected that this statistical width σ_{stat} will scale with current I as:

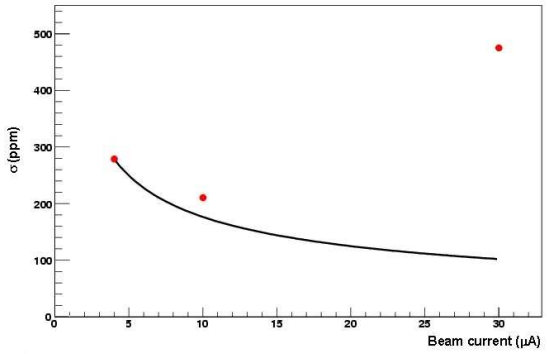

Figure 5: Combined Lumi asymmetry widths vs. current for a fan speed of 60 Hz and a 7mm x 7mm raster. Black line indicates results expected by counting statistics.

$$\sigma_{stat} \propto \frac{1}{\sqrt{I}}$$

At 30 μA, then, the expected statistical width is 121 ppm. The total measured width at 30 μA is 480 ppm. This value consists of the statistical width σ_{stat} and the width due to density fluctuations σ_{fluc} added in quadrature:

$$\sigma_{stat}^2 + \sigma_{fluc}^2 = \sigma_{total}^2$$

Subtracting the expected 121 ppm from the measured width in this fashion yields a density fluctuation width of 465 ppm. As seen from Figure 3, the problem continues to worsen at currents above 30 μA.

5.2 Fan speed

Figure 6 shows the regressed, normalized Lumi asymmetry widths for fan speeds of 40 and 60 Hz at a beam current of 35 μA and a target density of 0.136 g/cm^3 (the nominal density). All Lumis show fewer density fluctuations at the higher fan speed.

Figures 7 and 8 show Lumi widths for varied fan speeds at lower density targets (0.116 g/cm^3 and 0.083 g/cm^3, respectively). Again, higher fan speeds yield fewer density fluctuations, with the effect leveling off at high (60 to 70 Hz) speeds. Lower density results in more fluctuation, as can be seen by comparing the scales in figures 6, 7, and 8.

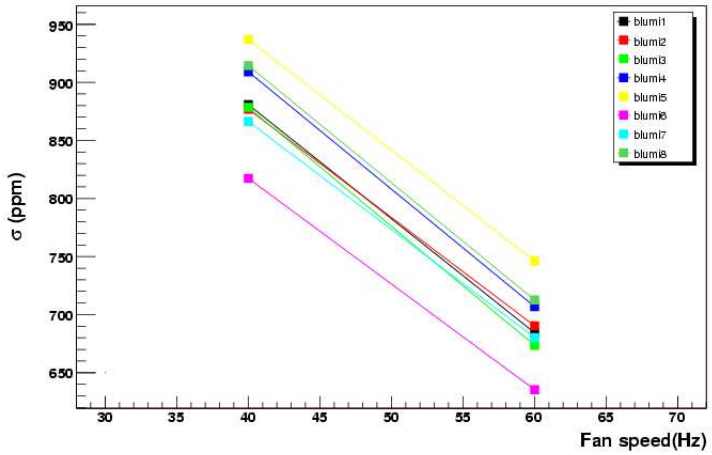

Figure 6: Lumi asymmetry widths vs. fan speed for a beam current of 35 μA, density 0.136 g/m^3, and a 7mm x 7mm raster.

The sensitivity of the widths to fan speed supports the idea that the broadening of the asymmetry distributions is due to target density fluctuations and not some other cause. If the source of the noise were located in the electron beam or the detectors themselves, then varying the fan speed (a property of the target only) would have no effect. Faster fan speeds circulate the helium throughout the cell more quickly, reducing localized heating and minimizing density fluctuations. The effect of target density on asymmetry widths also supports this idea.

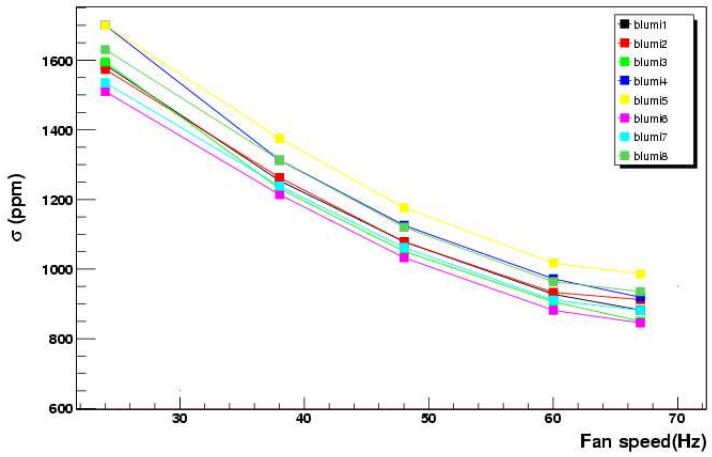

Figure 7: Lumi asymmetry widths vs. fan speed for a beam current of 35 μA, density 0.116 g/m^3, and a 7mm x 7mm raster.

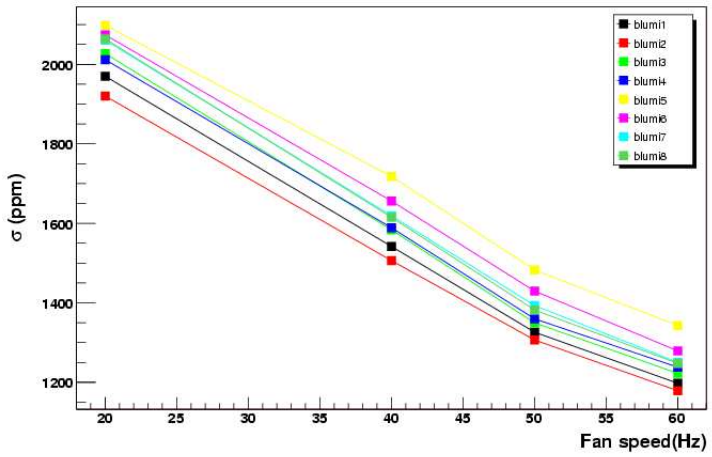

Figure 8: Lumi asymmetry widths vs. fan speed for a beam current of 35 μA, density 0.083 g/m^3, and a 7mm x 7mm raster.

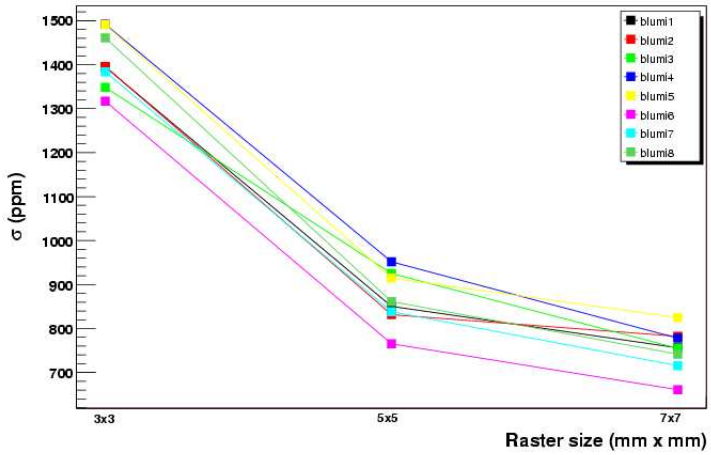

Figure 9: Lumi asymmetry widths vs. raster size for a 35 μA current and a 60 Hz fan speed.

5.3 Raster size

Figures 9 and 10 show the measured Lumi widths for different raster settings at 35 μA and 10 μA, respectively. As can be seen from Figure 8, density fluctuations decrease sizably as the raster increases at a "normal" operating current of 35 μA. This is due to the fact that less localized heating of the gas occurs with a larger raster. Figure 10 shows less dependence on raster size, which provides further indication that few density fluctuations occur at low current.

6 Implications for the Happex experiment

It has been shown that target density fluctuations are large at high current, low fan speed, and small raster. The fan speed and raster size can, for the most part, be chosen to minimize fluctuations. Lowering the beam current, however, causes the experiment to lose statistical accuracy since less scattering occurs. The issue then arises of how significantly target density fluctuations affect the asymmetry width as measured by the main detectors (Hall A high resolution spectrometers).

To address this, the intrinsic widths seen by the detectors are needed (with-

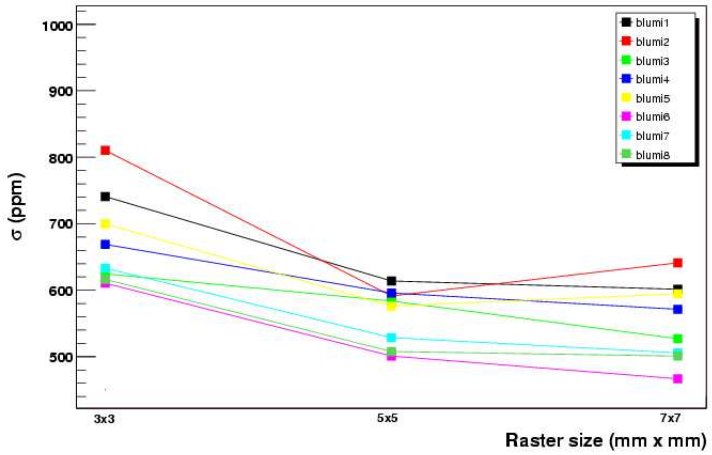

Figure 10: Lumi asymmetry widths vs. raster size for a 10 μA current and a 60 Hz fan speed.

out the contribution from target density fluctuations). These widths can be found by examining the widths of the distributions of the differences between detector asymmetries. By subtracting the detector asymmetries, any noise which is correlated in both detectors (like that caused by target density fluctuations) should be eliminated. The remaining widths should be those predicted by counting statistics.

To start with, the right detector asymmetries were subtracted from the left detector asymmetries. Figure 11 shows the width of this distribution for currents from 4 μA to 30 μA. The solid line shows the widths expected by Poisson distributions, with $\sigma_{stat} \propto \frac{1}{\sqrt{I}}$. The detector difference widths fall neatly on this line, indicating that target density fluctuations have indeed been subtracted. At 30 μA, the detector difference width is 2295 ppm. The width due to density fluctuations, derived earlier (see page 7), is σ_{fluc} =465 ppm.

The intrinsic width $\sigma_{intrinsic}$ can be added to the width due to target density fluctuations σ_{fluc} to get a total width σ_{total}:

$$\sigma^2_{intrinsic} + \sigma^2_{fluc} = \sigma^2_{total}$$

With $\sigma_{intrinsic} = 2295$ ppm and $\sigma_{fluc} = 465$ ppm, $\sigma_{total} = 2342$ ppm. This is an increase of 2% over the intrinsic widths.

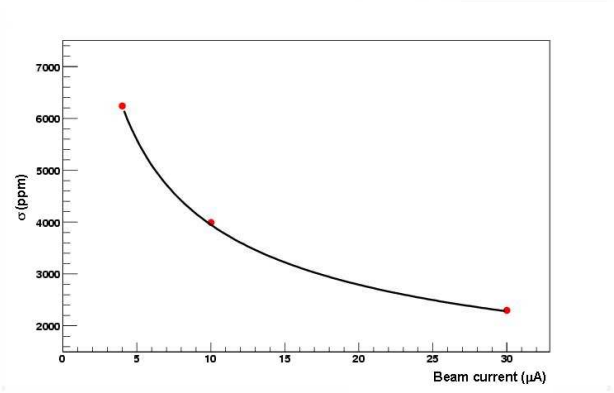

Figure 11: Detector difference asymmetry widths for a current scan. Fan speed is 60 Hz and raster setting is 7mm x 7mm. The expected counting statistics values are shown by a smooth black line.

7 Conclusions

Target density fluctuations increase the intrinsic widths measured by the Happex detectors by 2% at 30 μA beam current, 60 Hz fan speed, and a 7mm x 7mm raster size. This difference is compensated by the improvement in statistical accuracy because of the large number of interactions detected at 30 μA instead of 10 μA. At much higher currents, density fluctuations may be confounding enough to make the higher current unfavorable, but Lumi studies at currents over 30 μA would be necessary to determine this. A 7mm x 7mm raster and 60 Hz fan speed should be used for optimal statistical accuracy.

The reported worsening of statistics could be an exaggeration if density fluctuations are not constant throughout the length of the target cell. It is believed that beam-induced heating of the thin aluminum walls of the cell may increase fluctuations near the entrance and exit windows. This would increase the difference in sensitivity to density fluctuations between the Lumis and the main detectors. The main detectors, at a scattering angle of 6° [2], primarily accept electrons scattered from the middle of the cell. The back Lumis, at a smaller scattering angle of 0.5° to 0.8°, receive more electrons scattered from the entrance and exit windows. If these are the locations where target density fluctuations primarily take place, then the Lumis will be much more sensitive to those fluctuations than the main detectors [3][10].

References

[1] K.A. Aniol *et al.*, Phys. Rev. C **69**, 065501 (2004).

[2] D. Armstrong and R. Michaels, spokespersons, He4 Parity Experiment No. E00-114.

[3] D. Armstrong, Private communication (July 2005).

[4] R. Suleiman, "Hall A Luminosity Detector," (August 2004) (unpublished).

[5] D. Armstrong, B. Moffit, R. Suleiman, "Target Density Fluctuations and Bulk Boiling in the Hall A Cryotarget," Tech Note JLAB-TN-03-017, 2003.

[6] J. Cohen-Tanugai *et. al*, "Optical Properties of the DIRC Fused Silica Cherenkov Radiator," SLAC, Feb. 2001.

[7] R. Suleiman, "A Conceptual Design of Hall A Lumi Monitor," (August 2002) (unpublished).

[8] R. Suleiman, Private communication (July 2005).

[9] L. Lyons, "Statistics for nuclear and particle physicists," Cambridge: Cambridge University Press; 1986.

[10] K. Paschke, Private communication (July 2005).